

RUNAWAY CONTROL IN TOKAMAK DISCHARGES

R. Martin-Solis, R. Sanchez, B. Esposito ¹, J.D. Alvarez and L. Garcia

Universidad Carlos III de Madrid, C/Butarque 15, Leganes, 28911-Madrid, Spain.

¹ *Associazione Euratom-ENEA CRE, 00044-Frascati, Italy.*

Abstract

A test particle description of the runaway electron dynamics [1] is used to analyze the effect of the synchrotron radiation losses on the critical electric field for runaway generation. The model is extended to determine the influence of anomalous radial runaway losses on the critical electric field and the runaway energy. The above description of the runaway dynamics, together with a simple model for runaway production during a disruption, allows to estimate disruption generated runaway energies. The question of whether a resonance between the electron gyromotion and the harmonics of the toroidal field ripple can create an energy barrier in a tokamak during a disruption is also discussed.

1. Critical Electric Field for Runaway Generation

Consideration of the dynamics of relativistic runaway electrons, under electric field acceleration and collisions with the bulk plasma, leads to the conclusion [2] that there is a critical electric field $E_R = e^3 n_e \ln \Lambda / (4\pi \epsilon_0^2 m_e c^2)$ below which runaway generation is not possible. However, energy and momentum losses associated to the electron synchrotron radiation can give rise to more restrictive conditions for runaway generation and therefore to a critical electric field larger than E_R . Thus, the runaway electron dynamics has been analyzed using the test particle equations [1]:

$$\frac{dp_{\parallel}}{dt} = eE_{\parallel} - F_S \frac{p_{\parallel}}{p} - \frac{n_e e^4 \ln \Lambda m_e}{4\pi \epsilon_0^2} \gamma (Z_{eff} + 1 + \gamma) \frac{p_{\parallel}}{p^3}, \quad (1)$$

$$p_{\perp} \frac{dp_{\perp}}{dt} = -F_S \frac{p_{\perp}^2}{p} + \frac{n_e e^4 \ln \Lambda m_e}{4\pi \epsilon_0^2 p} \left(\gamma (Z_{eff} + 1 + \gamma) \frac{p_{\parallel}^2}{p^2} - \gamma^2 \right), \quad (2)$$

where p_{\parallel} is the electron momentum parallel to the magnetic field, p_{\perp} is the perpendicular electron momentum, and p is the total electron momentum; E_{\parallel} is the toroidal electric field and γ the relativistic gamma factor. The first term in Eq. (1) is the acceleration due the toroidal electric field, while the last term in (1) and (2) includes the effect of the collisions with the plasma particles. The radiation losses are described by means of the decelerating force, $F_S = \frac{2}{3} r_e m_e c^2 \left(\frac{v}{c}\right)^3 \gamma^4 \left\langle \frac{1}{R^2} \right\rangle$ (r_e is the classical electron radius and $\langle 1/R^2 \rangle$ gives the radius of curvature averaged over one gyrorotation).

The system of Equations (1) and (2) has in $(p_{\parallel}, p_{\perp}^2)$ space two singular points (a saddle point and a stable focus) with a well defined physical meaning [1]: the energy at the saddle point constitutes an estimate of the critical energy for runaway generation while the energy at the stable focus represents a limit for the runaway energy. Fig. 1 shows, for given plasma parameters, the relation between the normalized electric field $D = E_{\parallel}/E_R$ and the relativistic gamma factor γ_s at the singular points ($\dot{p}_{\parallel} = \dot{p}_{\perp} = 0$). For each value of D , there are two values of γ_s corresponding to such singular points: branch I in Fig. 1 gives γ_s at the saddle point, while branch II gives the electron gamma value at the stable focus. When D decreases, the value of

γ at the saddle point increases and its value at the stable focus decreases until both of them coalesce for a given value of D (the minimum of D vs. γ_s) which sets the critical electric field below which no electrons run away. Thus, the critical electric field for runaway generation can be deduced from the condition $dD/d\gamma_s = 0$. On the other hand, the radiation strength can be described by the dimensionless parameter $F_{gy} = 2\varepsilon_0 B_0^2 / 3n_e \ln \Lambda m_e$ (B_0 is the toroidal magnetic field) [1], so that the most noticeable radiation effects on the critical electric field are expected at high values of F_{gy} (i.e., at low densities and high B_0 values). In Fig. 2, the normalized critical electric field is plotted as function of the electron density and for different values of the effective ion charge Z_{eff} : due to the synchrotron radiation losses, the critical electric field for runaway generation becomes larger than E_R ($D > 1$), the most important effects taking place at low densities (higher F_{gy}). High Z_{eff} values, enhancing the collisional pitch angle scattering and therefore the radiation associated to the electron gyromotion, lead to larger deviations from E_R .

2. Radial Runaway Losses

Loss mechanisms which can deplete the runaway population, such as turbulent diffusion processes, can have an influence on the limiting runaway energy and the critical electric field for runaway generation. To quantify the effect of the radial diffusion losses on the runaway dynamics, a friction force $\vec{F}_D = -\vec{p}/\tau_D$, has been included in the test relaxation equations, where τ_D is the characteristic radial diffusion time, $\tau_D = a^2/5.8D_r$ (a is the plasma minor radius and D_r the runaway radial diffusion coefficient). The results are illustrated in Fig. 1, in which the normalized electric field is plotted versus γ_s for a case with no radial diffusion ($D_r = 0$) and two cases with radial diffusion coefficients $D_r = 0.5$ and $1 \text{ m}^2/\text{s}$, respectively. Radial diffusion losses have two main consequences on the runaway dynamics: (i) a reduction in the limiting runaway energy (branch II in Fig. 1); (ii) an increase in the critical electric field (minimum of D vs. γ_s).

Runaway electrons are particularly sensitive to magnetic fluctuations, which lead to anomalous radial runaway losses described by a radial diffusion coefficient, $D_r \approx \pi q R_0 c (b_r/B_0)^2$ (q is the safety factor, R_0 the major radius and b_r/B_0 the normalized radial magnetic fluctuations). In Fig. 3, the critical electric field for runaway generation is plotted as function of the magnetic fluctuation level b_r/B_0 for typical plasma conditions during a disruption in JET and ITER. It is found that a magnetic fluctuation level above $(b_r/B_0) > 10^{-3}$ may be enough to block runaway generation in these devices during a disruption. Observations of runaway generation suppression due to enhanced magnetic fluctuations have been reported during disruptive discharge-terminations in JT-60U [3].

3. Disruptions and Runaways

A simple model for runaway production during a disruption, including both the Dreicer and the secondary generation processes, will be used to predict the energy reached by disruption generated runaway electrons. This model essentially assumes that the current carried by the runaway electrons replaces the plasma current I_p , therefore reducing the electric field until it vanishes [4]. Thus, the formation of the runaway current during the disruption current quench is described by the following set of equations:

$$E_{\parallel} = -\frac{L}{2\pi R_0} \frac{dI_p}{dt} = \eta(j_p - j_r); \quad \frac{dn_r}{dt} = n_e \nu_0 \lambda(\varepsilon) + \frac{n_r}{\tau_r} \left(\frac{E_{\parallel}}{E_R} - 1 \right) \quad (3)$$

Here L is the internal inductance, η the Spitzer resistivity, $j_p = I_p/\pi a^2 k$ the plasma current density (k is the plasma elongation), n_r the runaway density and j_r the runaway current density, $j_r = ecn_r$. The first contribution to dn_r/dt in (3) describes the Dreicer generation: ν_0 is the collision frequency, λ is the runaway birth parameter, and $\varepsilon = (E_{||}/E_R)(kT_e/m_e c^2)$. The second contribution corresponds to the secondary generation mechanism, with $\tau_r = (4\pi\varepsilon_0^2 m_e^2 c^3 / e^4 n_e) \sqrt{3(5 + Z_{eff})/\pi}$. The results of the model depend critically on the parameter ε (i.e., on $E_{||}$, n_e and T_e) and are illustrated in Figs. 4 and 5 for a 5 MA JET disruption ($R_0 = 3$ m, $a = 1$ m, $n_e = 1 \times 10^{20} \text{ m}^{-3}$, $Z_{eff} = 3$, $T_e = 5$ eV, and $L \simeq 4 \mu\text{H}$). Fig. 4 (a) shows the calculated runaway current I_r vs. ε : the full line is obtained including the Dreicer and secondary generation processes, and the dashed line considering only Dreicer generation.

Combination of Eq. (3) with the single particle equations (1) and (2) allows to estimate the runaway energy. The maximum energy E_{max} that an individual runaway can reach, the average runaway energy E_{av} , and the total energy content E_b in the runaway beam are given as function of ε in Figs. 4 (b) and 5 (b). As pointed out in [4], secondary generation enhances the runaway production, reducing the time during which $E_{||}$ is high, so that the runaway current is maximized and the runaway energy is reduced. Moreover, Dreicer generation results in a monoenergetic runaway beam ($E_{max} \approx E_{av}$) while, at low ε , secondary generation leads to an exponential distribution function ($E_{av} \ll E_{max}$) so that, at low ε values, the reduction in the average and beam energies ($E_b \approx I_r E_{av}$) is even larger than for E_{max} .

A resonance between the electron gyromotion and the harmonics of the toroidal field ripple can set an additional barrier on the maximum runaway energy. The interaction with the n th harmonic of the toroidal field ripple takes place at an electron energy $E_n \simeq eB_0 R_0 c / n N_c$ (N_c is the number of toroidal field coils and n the toroidal harmonic number), and has been implemented in the test particle dynamics following [1]. The efficiency of the resonant interaction is strongly dependent on the ripple amplitude. Fig. 5 (a) shows the minimum (normalized) ripple amplitude $\delta B_{up}/B_0$ required for an efficient blocking of the maximum runaway energy as function of ε and for $n = 1 - 3$. The main conclusions can be summarized as follows: (i) the strongest runaway-ripple interaction (lowest δB_{up} required) takes place at the lowest harmonics; (ii) δB_{up} decreases with increasing ε as the runaway production is then larger and the electric field lower, being the electrons more easily stopped at the resonance; (iii) for secondary generation, ripple resonance effects are only expected at low ε , when E_{max} is larger than the resonant energies; however, due to the exponential nature of the runaway distribution function at low ε , only a small fraction of the runaway population (at the highest energies) will be affected and the total energy of the runaway beam will not be substantially changed. For Dreicer generation, the effects are larger due to the higher runaway energies and, as $E_{av} \approx E_{max}$, E_b may noticeably change: Fig. 5 (b) illustrates the effect on E_b , assuming only Dreicer generation, of the interaction with the $n = 1$ ripple harmonic in JET ($N_c = 32$, $E_{n=1} \simeq 84$ MeV).

References

- [1] R. Martin-Solis, J.D. Alvarez, R. Sanchez and B. Esposito: *Proc. 24th EPS Conference on Controlled Fusion and Plasma Physics*, Berchtesgaden, Vol. **21A**, Part II, p. 865 (1997).
- [2] J.W. Connor and R.J. Hastie: *Nucl. Fusion* **15**, 415 (1975).
- [3] Y. Kawano, R. Yoshino, Y. Neyatani et al.: *Proc. 24th EPS Conference on Controlled Fusion and Plasma Physics*, Berchtesgaden, Vol. **21A**, Part II, p. 501.

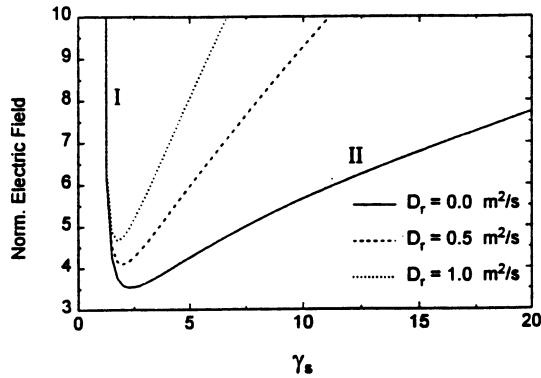


Fig.1: Normalized electric field vs. γ_s at the singular points. Full line: no radial diffusion assumed ($D_r = 0$); dashed line: $D_r = 0.5 \text{ m}^2/\text{s}$; dotted line: $D_r = 1 \text{ m}^2/\text{s}$. Plasma parameters: $B_0 = 3 \text{ T}$, $R_0 = 3 \text{ m}$, $a = 1 \text{ m}$, $n_e = 0.5 \times 10^{19} \text{ m}^{-3}$, $Z_{eff} = 3$.

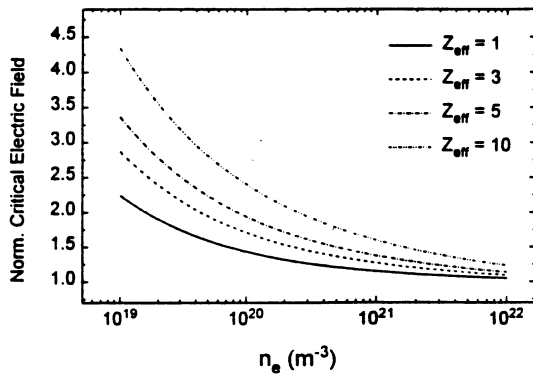


Fig.2: Normalized critical electric field vs. electron density for $Z_{eff} = 1, 3, 5, 10$. Toroidal magnetic field: $B_0 = 3 \text{ T}$.

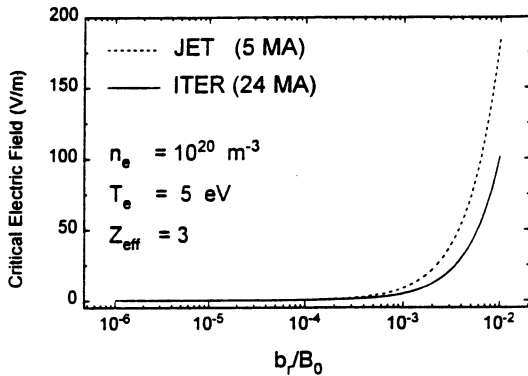


Fig.3: Critical electric field vs. radial magnetic fluctuation level for typical plasma parameters during a disruption in JET ($B_0 = 3 \text{ T}$, $R_0 = 3 \text{ m}$) and ITER ($B_0 = 5.68 \text{ T}$, $R_0 = 8.14 \text{ m}$).

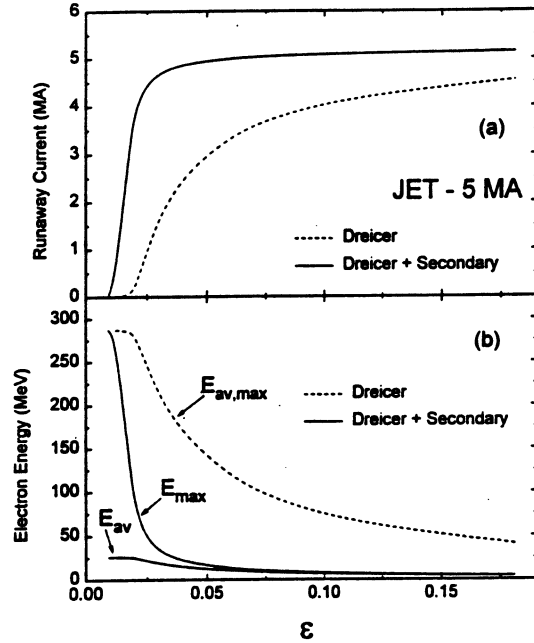


Fig.4: Predictions of the disruption model for a 5 MA JET disruption: (a) Runaway current vs. ϵ ; (b) Maximum and average runaway energies vs. ϵ . Full lines: Dreicer and secondary generation; dashed lines: Dreicer generation.

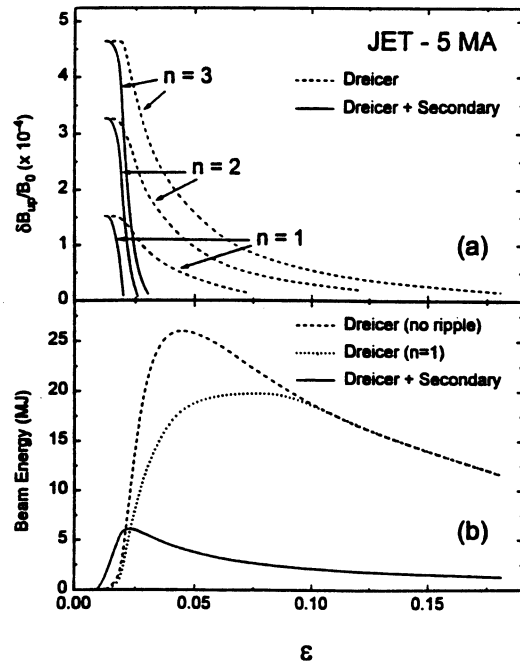


Fig.5: For the same example that Fig.4: (a) Minimum (normalized) ripple amplitude $\delta B_{up}/B_0$ for efficient runaway-ripple interaction vs. ϵ ($n = 1 - 3$); (b) Total energy in the runaway beam vs. ϵ (full line: Dreicer and secondary generation; dashed line: Dreicer generation; dotted line: Dreicer generation and interaction with the $n = 1$ ripple harmonic).